# Journal of Materials Chemistry A



### COMMUNICATION

View Article Online



Cite this: DOI: 10.1039/d0ta05258b

Received 23rd May 2020 Accepted 17th June 2020

DOI: 10.1039/d0ta05258b

rsc.li/materials-a

# Breaking the short-range proximity requirement in quantum dot/molecular catalyst hybrids for CO<sub>2</sub> reduction *via* long-range hot electron sensitization†

The efficient light-driven fuel production from homogeneous photocatalytic systems is one promising avenue towards an alternative energy economy. However, electron transfer from a conventional photosensitizer to a catalyst is short-range and necessitates spatial proximity between them. Here we show that energetic hot electrons generated by Mn-doped semiconductor quantum dots (QDs) allow for long-range sensitization of Ni(cyclam)-based molecular catalysts, enabling photocatalytic reduction of  $CO_2$  to CO without requiring chemical linkages between the QDs and catalyst molecules. Our results demonstrate the potential of hot electron sensitization in simplifying the design of hybrid catalyst systems while improving photocatalytic activity.

#### Introduction

Hybrid photocatalytic systems, constructed from a photosensitizing unit (PU) and a catalyst, have been extensively studied for homogeneous photocatalytic conversions of energy relevant small molecules to generate hydrogen ( $H_2$ ) and reduction products of carbon dioxide ( $CO_2$ ). For the homogeneous light-driven reduction of  $CO_2$ , hybrid systems employing molecular catalysts, such as Ni(cyclam) and Fe(porphyrin), have been studied in combination with either molecular photosensitizers, like  $Ru(bpy)_3^{2+}$  and  $Ir(ppy)_3$ , as well as semiconductor quantum dots (QDs).

In contrast to utilizing molecular photosensitizers, QD/molecular catalyst hybrid systems take advantage of the

comparatively higher photostability and larger absorption cross section of QDs for photosensitization, thereby "powering" the molecular catalyst for precise and selective catalytic reactions more effectively. However, all two-component photocatalytic systems require, at least temporarily, proximity between the PU (in its excited or reduced state) and the catalysts molecules (precatalysts and all catalyst intermediates) for productive electron transfer to be possible. One route to overcoming this inherent limitation, is the use of synthetic chemistry to link both components together. Examples of this approach include the covalent attachment of catalysts to the PU,10 as well as the utilization of supramolecular interactions, such as van der Waals interaction,11 hydrogen bonding,12 and ion pairing.13 For example, in a report by Weiss et al. it was shown that ion pairing between anionically terminated II-VI QDs and synthetically modified, highly cationic Fe(porphyrin) catalysts, allowed for a significant increase in CO2 conversion to carbon monoxide (CO).13

Although these approaches are certainly promising, they add complexity, require additional synthetic steps, may not be applicable to a large variety of catalysts, and given the sensitivity of molecular catalysts performance to ligand design, may not allow to tune catalyst and PU independently from each other. We propose that the burden of linking QDs and molecular catalyst can potentially be alleviated by using hot electrons which would enable long-range electron transfer for sensitization of molecular catalysts that are separated far from the QDs. Since hot electrons can transfer across a thick and high-energy barrier, QD sensitizer and molecular catalyst do not necessarily need to be linked as tightly in space. Recently, the generation of hot electrons with excess kinetic energies of more than 2 eV above the conduction band edge was demonstrated via excitonto-hot electron 'upconversion' under weak visible excitation conditions in Mn-doped II-VI QDs.14-16 The exciton-to-hot electron upconversion is achieved through a sequential twophoton process, mediated by the long-lived excited ligand field state of Mn<sup>2+</sup> as the intermediate state that adds excess energy to the electrons in the conduction band. These hot

<sup>&</sup>quot;Department of Chemistry, Texas A&M University, College Station, Texas 77843, USA. E-mail: dhson@chem.tamu.edu; nippe@chem.tamu.edu

<sup>&</sup>lt;sup>b</sup>Center for Nanomedicine, Institute for Basic Science (IBS) and Graduate Program of Nano Biomedical Engineering, Advanced Science Institute, Yonsei University, Seoul 03722, Republic of Korea

 $<sup>\</sup>dagger$  Electronic supplementary information (ESI) available: Experimental details, quantum efficiency calculations, and additional spectra. See DOI: 10.1039/d0 t a 05258b

<sup>‡</sup> These authors contributed equally to this work.

electrons can transfer across a 7 nm-thick insulating Al<sub>2</sub>O<sub>3</sub> layer in an electrochemical cell platform, 17 and even create photoelectron emission current under vacuum condition,18 demonstrating their ability to travel long distances over the high energy barrier. Therefore, hot electrons generated in Mn-doped QDs are expected to overcome the shortcomings of short-range interfacial electron transfer of band edge electrons that limits the spatial extent of catalytic reactions to the immediate proximity of the QD surface. Compared to plasmonic hot electrons in metal nanostructures, the absolute energy of hot electrons from upconversion is several eV higher.<sup>18</sup> The advantage of these hot electrons in QD-based photocatalysis was recently demonstrated for photocatalytic H<sub>2</sub> production with Mn-doped QDs in the absence of a molecular catalyst or other cocatalyst.19 Based on our studies on hot electron photocurrent in an electrochemical cell and hot electron-induced H2 generation discussed above, we estimate that the length scale of hot electron transfer can readily be in the range of 5-10 nm and will depend on the specific chemical environment.

Building on these results, the present study establishes the feasibility of using hot electrons for long-range sensitization of molecular catalysts in "non-linked" QD/molecular catalyst hybrid systems. We show that for simple QD/molecular catalyst (precatalyst is [Ni(cyclam)]<sup>2+</sup>) mixtures, both CO<sub>2</sub> to CO conversion (under a CO2 atmosphere) and H2 production (under an Ar atmosphere) are strongly enhanced if Mn-doped QDs are employed as the PUs as compared to those using undoped QDs (Chart 1). The comparison of CO production rates of Mn-doped QD/[Ni(cyclam)]2+ and undoped QD/ [Ni(cyclam)]<sup>2+</sup> systems strongly suggests that long-range hot electron sensitization is indeed possible, resulting in a 6-fold increase in the production of CO from CO<sub>2</sub> of the former under otherwise identical conditions. The results from this study clearly demonstrate the benefits of hot electron sensitization in non-linked hybrid systems, which will greatly simplify the design and construction of hybrid photocatalysts by eliminating the need for linkages between PUs and molecular catalysts.

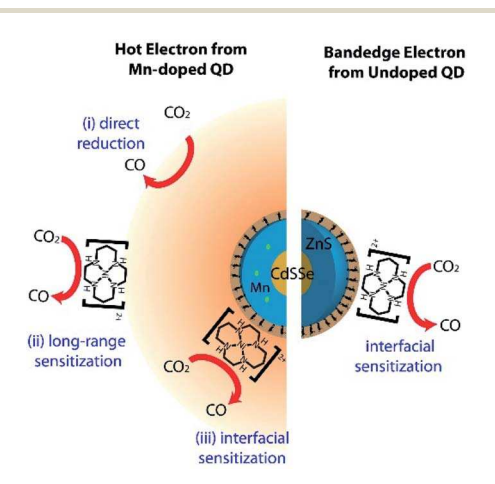


Chart 1 Potential CO generation pathways for doped (left) and undoped (right) QDs in QD/catalyst systems. See text for discussion of pathways (i–iii).

#### Results and discussion

In this work, we used Mn-doped and undoped CdSSe/ZnS core/ shell QDs of the same size and host structure as the source of hot electrons and band edge electrons, 20 respectively, to examine the capability of hot electrons to perform long-range sensitization of [Ni(cyclam)]2+ in a non-linked hybrid photocatalyst system. We chose [Ni(cyclam)]<sup>2+</sup> as a molecular catalyst as Ni(cyclam)-based catalysts are well known to display good selectivity for CO2 to CO conversion under electro-21 and photocatalytic3 conditions while also being able to catalyse H2 production in the absence of CO<sub>2</sub>.<sup>22</sup> Fig. 1 shows the absorption and photoluminescence (PL) spectra of Mn-doped and undoped QDs as well as their TEM images. Both Mn-doped and undoped ODs have nearly identical absorption spectra and extinction coefficient, ascertaining the same amount of light absorption for a given concentration of QDs in solution (see ESI for details†). Exciton PL is centred at 487 nm for both Mn-doped and undoped QDs, while only Mn-doped QDs show PL near 600 nm from  ${}^4T_1 \rightarrow {}^6A_1$  ligand field transitions from Mn excited states. Both, Mn-doped and undoped QDs, exhibit comparable total PL quantum yields of 50-60%.

In order to assess the capability of hot electrons to perform long-range sensitization of  $[Ni(cyclam)]^{2+}$  for  $CO_2$  reduction, we compared the catalytic activity for CO production for four different catalyst systems in  $CO_2$ -saturated aqueous media: (i) undoped QD only, (ii) undoped QD/ $[Ni(cyclam)]^{2+}$ , (iii) Mndoped QD only, (iv) Mn-doped QD/ $[Ni(cyclam)]^{2+}$ . For all four systems, the molar concentration of QDs were  $\sim 20~\mu M$  and 0.77 M triethylamine (TEA) was used as the sacrificial hole scavenger (see Experimental for details†). Solutions in the photocatalytic reactor were illuminated using an LED (450 nm, 0.1 W cm $^{-2}$ ) to excite the QDs near the bandgap (Fig. S1†). While  $[Ni(cyclam)]^{2+}$  has an absorption at 450 nm (Fig. S2†), it

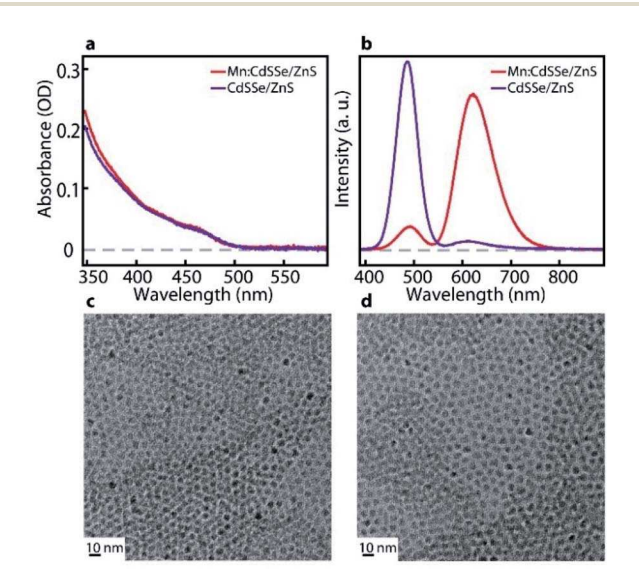


Fig. 1 Absorption (a) and PL (b) spectra of Mn-doped (red) and undoped (purple) CdSSe/ZnS QDs before adding TEA and [Ni(cyclam)]<sup>2+</sup>. TEM of Mn-doped (c) and undoped (d) QDs.

does not affect the comparison of the sensitization of nonlinked [Ni(cyclam)]<sup>2+</sup> by hot electrons from Mn-doped QDs and band edge electrons from undoped QDs.

Fig. 2 shows the amounts of CO and H<sub>2</sub> produced for the four different photocatalyst systems as a function of irradiation time up to 8 hours. Table 1 summarizes the total amount of CO and H<sub>2</sub> produced after 8 h of reaction and their ratio. In the absence of [Ni(cyclam)]<sup>2+</sup>, undoped QDs did not result in detectable gaseous products with CO and H2 being below the detection limit. The undoped QD/[Ni(cyclam)]2+ system display an increase in the production of both, CO and H<sub>2</sub>, with a CO: H<sub>2</sub> ratio of 0.76: 1. Given the absence of appreciable amounts of CO in the absence of [Ni(cyclam)]<sup>2+</sup>, CO was likely produced via the short-range sensitization of [Ni(cyclam)]<sup>n+</sup> by band edge electrons. In this case, the sensitization can only occur for those  $[Ni(cyclam)]^{n+}$  molecules sufficiently close to the surface of the QDs. In contrast to undoped QDs, Mn-doped QDs are able to produce CO even in the absence of [Ni(cyclam)]<sup>2+</sup> with an activity comparable to that of the undoped QDs/[Ni(cyclam)]<sup>2+</sup> system. However, the major product under these conditions is  $H_2$ , yielding a CO:  $H_2$  product selectivity of 0.07: 1.

Importantly, the efficiency and selectivity for CO production are greatly improved in Mn-doped QD/[Ni(cyclam)]<sup>2+</sup> system. A 6-fold enhancement for CO production is observed when compared to either undoped QD/[Ni(cyclam)]<sup>2+</sup> system or Mndoped QD only. The CO: H2 ratio of 1.05:1 is favoring the production of CO. These improvements suggest that sensitization of  $[Ni(cyclam)]^{2+}$  by hot electrons is  $\sim 6$  times more efficient than by band edge electrons if the small contribution from the direct reduction of CO<sub>2</sub> to CO by Mn-doped QDs is ignored. The increase in efficiency of the sensitization by hot electrons is the combined result of the enhanced electron transfer rate to [Ni(cyclam)]<sup>2+</sup> at a given distance and the longer electron

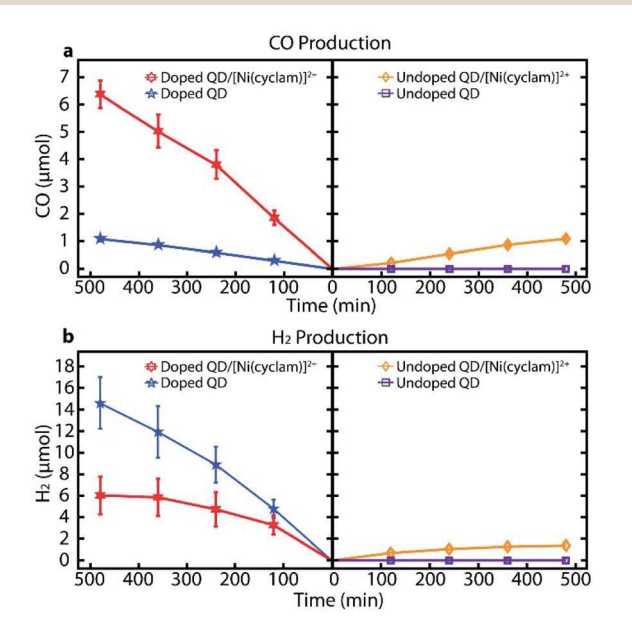


Fig. 2 Comparison of photocatalytic CO (a) and H<sub>2</sub> (b) production under a CO<sub>2</sub> atmosphere, using Mn-doped (left) or undoped QDs (right) in the presence or absence of [Ni(cyclam)]<sup>2+</sup>.

Table 1 CO and H<sub>2</sub> production by four different catalyst combinations under CO2 atmosphere after 8 h of reaction

Catalyst combination	CO (µmol)	$H_2$ ( $\mu mol$ )	CO: H <sub>2</sub> ratio
Undoped QD only	$0^a$	$0^a$	_
Undoped QD/[Ni(cyclam)] <sup>2+</sup>	1.0	1.3	0.76:1
Mn-doped QD only	1.0	14.6	0.07:1
Mn-doped QD/[Ni(cyclam)] <sup>2+</sup>	6.3	6.0	1.05:1
<sup>a</sup> Below detection limit.			

transfer distance of hot electrons. In a simplified picture, one may view the enhancement of sensitization as the larger spatial extent of sensitization by hot electrons giving access to more remotely located molecular catalysts. Several control experiments were carried out to validate our interpretations: (1) saturating post-CO<sub>2</sub> reduction solutions with Ar and continuing irradiation did not result in any CO formation for either test system, and confirms that CO production originates solely from the reduction of CO<sub>2</sub>. (2) Addition of the nickel salt Ni(BF<sub>4</sub>)<sub>2</sub>-·6H<sub>2</sub>O instead of [Ni(cyclam)]<sup>2+</sup> rapidly resulted in a grey precipitate (likely colloidal Ni particles) under irradiation with no detectable formation of CO and H2, which strongly suggests that the molecular nature of  $[Ni(cyclam)]^{n+}$  remains intact during catalysis and it is acting as the active catalyst. (3) Irradiation of [Ni(cyclam)]<sup>2+</sup> in the absence of either QD did not result in H<sub>2</sub> or CO production. (4) Irradiation of Mn-doped QDs in the presence of only "free" cyclam ligand did not increase catalytic activity as compared to entry 3 in Table 1.

Quantitative estimations of the enhancement of sensitization by each hot electron is difficult, because of the uncertainty in the quantum efficiency (QE) of hot electron generation from exciton-to-hot electron upconversion. In our earlier study that used Mn-doped QDs for hot electron-driven H<sub>2</sub> production, the upper limit to the QE of generating hot electron was estimated  $\sim$ 20% for that particular QD structure. This suggests that each hot electron from Mn-doped QDs can be an order of magnitude more efficient in sensitizing unbound [Ni(cyclam)]2+ than the band edge electrons from undoped QDs. In this study, we focus on firm experimental verification of the effectiveness of hot electron sensitization in non-linked hybrid catalyst systems for photocatalytic reduction. Detailed quantitative assessment and optimization of the overall efficiency of photocatalytic reduction via hot electron sensitization, dictated by the hot electron generation efficiency of the QD itself and other environmental variables will be addressed in future studies.

Although the presented results are obtained for not vigorously optimized conditions, we estimate the QE of CO and H<sub>2</sub> production by hot electrons in Mn-doped QD/[Ni(cyclam)]<sup>2+</sup> (see ESI for details†). Assuming that the majority of reaction products are formed through hot electrons, we estimate a QE for CO production to be approximately 0.04%, with nearly the same QE for H<sub>2</sub> production for the Mn-doped QD/[Ni(cyclam)]<sup>2+</sup> system under our experimental conditions. This QE is on the same order of magnitude as those for non-linked two component  $Ru(bpy)_3^{2+}/[Ni(cyclam)]^{2+}$  hybrid systems (0.06%) studied earlier.23 However, since it is often difficult to make meaningful

direct comparisons of QE values between different photocatalytic systems from different studies, we will not put much emphasis on this comparison. Nevertheless, it is informative to compare the enhancement factor (6-fold) of CO production gained by hot electron sensitization in non-linked QD/[Ni(cyclam)]<sup>2+</sup> system in this study with the reported enhancement factor of CO production obtained by 'linking' undoped QDs and [Ni(cyclam)]<sup>2+</sup>. In a study by Reisner et al., it was shown that the covalent attachment of phosphonic acid-functionalized [Ni(cyclam)<sup>2+</sup>-derived catalysts to the surface of ZnSe QDs allowed for a 3-fold increase in photocatalytic CO production, as compared "non-linked" ZnSe QD/[Ni(cyclam)]<sup>2+</sup> mixtures.<sup>3</sup> Although detailed reaction conditions are different between the two hybrid catalyst systems, our results indicate that the net effect of hot electron sensitization in non-linked hybrid catalyst system is similar to that of forming chemical linkage between the sensitizer and molecular catalysts.

Chart 1 illustrates the differences in the pathways of [Ni(cyclam]<sup>2+</sup> sensitization and CO<sub>2</sub> to CO conversion by band edge electron and hot electrons from undoped and Mn-doped QDs respectively. Several pathways for CO generation in Mn-doped QD/[Ni(cyclam)]<sup>2+</sup> systems can be envisioned: (i) the direct reduction of CO2 to CO by hot electrons without involving the molecular catalyst, (ii) reduction via long-range sensitization of remote [Ni(cyclam)]<sup>2+</sup>, (iii) reduction via interfacial sensitization of [Ni(cyclam)]<sup>2+</sup> near the QD surface. Pathway (i) accounts for the production of CO from Mn-doped QDs in the absence of [Ni(cyclam)]<sup>2+</sup>. While no detailed mechanism is available, the involvement of solvated electrons, similar to those reported by Hamers et al.,24 is a possibility, since hot electrons from upconversion possessing >2 eV excess energy above the band edge could be injected into the solvent forming solvated electron. Considering the 6-fold increase in CO production in the presence of [Ni(cyclam)]<sup>2+</sup>, this direct reduction pathway likely has only a minor contribution to the product formation in the hybrid catalyst system. Since non-linked [Ni(cyclam)]<sup>2+</sup> molecules are distributed with varying distances from the QD surface, both long-range and interfacial sensitization are operating when Mn-doped QDs are used, whereas only interfacial sensitization is possible with undoped QDs. Since undoped QD/ [Ni(cyclam)]<sup>2+</sup> systems are 6 times less active than Mn-doped QD/[Ni(cyclam)]<sup>2+</sup> for CO production, pathway (iii) should also have minor contributions. Therefore, we conclude that longrange hot electron sensitization is the major pathway accounting for the enhanced CO production in Mn-doped QD/ [Ni(cyclam)]<sup>2+</sup> system.

To further support our conclusion, we also tested the photocatalytic  $H_2$  production ability of  $[Ni(cyclam)]^{2+}$  in the presence of either Mn-doped QDs or undoped QDs under Ar atmosphere. Although  $[Ni(cyclam)]^{2+}$  displays good selectivity for  $CO_2$  reduction in various media, it is also known to be a competent catalyst for  $H_2$  evolution in the absence of  $CO_2$ . Fig. 3 compares the amount of  $H_2$  produced for four different QD/catalyst combinations. In agreement with the above results for  $CO_2$  reduction, Mn-doped QD/ $[Ni(cyclam)]^{2+}$  system is superior to both Mn-doped QDs in the absence of catalyst and undoped  $QD/[Ni(cyclam)]^{2+}$  systems, displaying a 3-5-fold

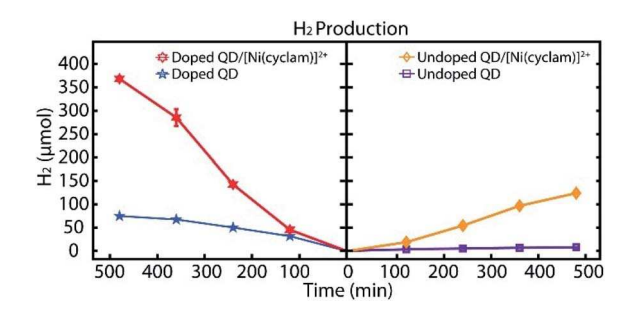


Fig. 3 Comparison of photocatalytic activity for  $H_2$  generation under Ar atmosphere using Mn-doped (left) or undoped QDs (right) in the presence or absence of  $[Ni(cyclam)]^{2+}$ .

enhancement of producing  $H_2$ . This result also indicates that the benefits of long-range hot electron sensitization can be universal and applicable to a wide range of photocatalytic reductions facilitated by non-linked hybrid catalyst systems.

#### Conclusions

In this work we showed that hot electron sensitization can be utilized to produce CO from CO<sub>2</sub> with QD/molecular catalyst hybrid systems without requiring a linkage between QDs and molecular catalysts. Mn-doped QDs generating energetic hot electrons could sensitize [Ni(cyclam)]<sup>2+</sup> in solution *via* longrange electron transfer, enabling CO<sub>2</sub> reduction. The results reveal a new avenue for the design of hybrid catalyst systems by removing the necessity of linkage and spatial proximity between photosensitizer and molecular catalysts.

## Experimental

#### Synthesis of [Ni(cyclam)](BF<sub>4</sub>)<sub>2</sub>

The [Ni(cyclam)](BF<sub>4</sub>)<sub>2</sub> was synthesized following a previously reported method.<sup>25</sup> Ni( $\pi$ ) tetrafluoroborate hexahydrate(0.8306 g) was dissolved in 40 mL of 30 °C ethanol. This solution was then added to a solution of cyclam (0.5000 g) dissolved in 20 mL of 30 °C ethanol. The resulting orange solid was filtered off, washed with cold ethanol, and allowed to dry overnight.

#### **QD Synthesis**

Mn-doped and undoped CdSSe/ZnS core/shell quantum dots (QDs) were synthesized following procedures published previously. <sup>26,27</sup> The sulfur/selenium (S/Se) precursor was prepared by adding 0.5 mL of a 1 M tributylphosphine (TBP) solution of selenium to a mixture of 10 mL of heated octadecene (ODE) and sulfur (0.081 g). Subsequently, 2 mL of S/Se precursor solution was swiftly injected to a solution of ODE (12 mL) with CdO (0.128 g) and oleic acid (2.1 mL) heated to 250 °C. After the injection, the reaction temperature was reduced to 240 °C and allowed to proceed for 70 seconds, which produced CdSSe core QDs. After quenching the reaction by rapid cooling of the reactant mixture, the produced QDs were precipitated by adding acetone and centrifugation. The precipitated CdSSe core QDs were recovered and dispersed in toluene. Three more cycles of

Communication

precipitation/redispersion were applied to further purify the ODs before coating ZnS shell.

Shell coating and Mn doping were performed following the previously reported procedure employing successive ionic layer adsorption and reaction (SILAR) method. The core QDs were initially dissolved in a mixture of ODE (6 mL) and oleylamine (2 mL) and heated up to 220 °C under  $\rm N_2$ . Subsequently, the mixture of ODE–sulfur (0.25 M) and the zinc precursor solution (0.25 M zinc stearate in toluene with 5% octylamine) were added dropwise to the core QD solution over 10 minutes. After adding two layers of ZnS shell, the 'intermediate' core/shell QDs were precipitated and purified following the same procedure of purifying the core QDs.

The purified 'intermediate' core/shell QDs were dispersed in the mixture of ODE (6 mL) and oleylamine (2 mL) and heated up to 260 °C for Mn-doping. Mn-doping was performed by adding ODE-sulfur solution and a solution of Mn(OAc)<sub>2</sub> (0.029 g) in oleylamine (6 mL) dropwise then cooling after 20 minutes. Subsequently, the Mn-doped QDs were purified using the same procedure described above and 4 additional ZnS shell layers were coated. The final Mn-doped CdSSe/Zn core/shell QDs were recovered and purified by applying multiple precipitation/redispersion cycles using methanol and toluene as anti-solvent and solvent. The final doping concentration calculated from ICP elemental analysis was 4.7%. For the undoped QDs the same procedure was followed excluding the Mn-doping step.

The resulting QDs (both Mn-doped and undoped core/shell QDs), initially passivated with oleylamine and dispersible in nonpolar solvent underwent ligand exchange with 4-mercaptopropionic acid (MPA) to make them water soluble. To the QDs dispersed in chloroform the mixture of water (0.200 mL), methanol (0.800 mL) and MPA (0.100 mL) was added. The pH of solution was maintained at >8 by adding small amount of NaOH. After stirring the mixture for 3 hours, the ligand-exchanged QDs in the organic phase had transferred to the aqueous phase. After separating the aqueous phase, the QDs were isolated by precipitating with acetone to remove any unbound MPA. The recovered QDs were dispersed in water before use.

The robustness of Mn-doped II–VI QDs important for the long-term catalytic activity has been well established previously. Diffusion of Mn<sup>2+</sup> ions within the QD lattice requires relatively high temperatures (e.g., >250 °C) to overcome strong Mn-chalcogen bonds, therefore Mn<sup>2+</sup> ions should remain stably within the QDs under the here employed photocatalysis conditions at ambient temperature. <sup>28,29</sup> To additionally confirm the stability of Mn<sup>2+</sup> ions within the QDs, we compared the ratio of Mn PL vs. exciton PL in Mn-doped QDs before and after photocatalysis. The comparison showed no significant change of PL intensity ratio, indicating no diffusion of Mn<sup>2+</sup> ions out of the QDs.

# Quantification of the photocatalytic reduction product (CO and $H_2$ )

The quantification of the gaseous photocatalytic reduction products (CO and  $H_2$ ) were performed using a custom-built

reactor and gas chromatography (GC) for detection. The cylindrically shaped reactor has the inner diameter of 5 cm with total internal volume of 150 cm $^3$ . The total volume of the reactant mixture is 60 mL (54 mL of DI water + 6 mL of triethylamine as the sacrificial hole scavenger). At the concentration of QDs of this study ( $\sim\!20~\mu\text{M}$ ), the absorbance of the QDs at the excitation wavelength (450 nm) is 0.04 in a 1 cm pathlength cuvette. The concentration of [Ni(cyclam)](BF\_4)\_2 dissolved in the solution is 3 mM.

The sealed reactor containing all the reactant mixture, as described above, was bubbled with either  $CO_2$  (for  $CO_2$  reduction) or Ar (for control experiment) for 40 min then placed in a circulated water bath to keep the temperature of the reactor constant at 25 °C. A blue 450 nm LED was used as the excitation source. A 200  $\mu$ L aliquot of the headspace was taken every 2 h (2, 4, 6 and 8 h) with a gas tight syringe (Gas Syringe Series A-2 Luer Lock 500  $\mu$ L RN, VICI precision sampling) for the analysis of the concentration of the product gas. The analysis was performed on a GC with a thermal conductivity detector (for  $H_2$  detection) and flame ionization detector equipped with a methanizer (for CO detection).  $CH_4$  was used as an internal standard to check the potential variation during the sampling and injection of the aliquots.

The calibration of the detectors for the quantification of CO and  $H_2$  was done in the following way after the completion of each experiment. The reactor was first purged with  $CO_2$  for 30 minutes to remove all CO,  $H_2$ , and  $CH_4$ . This was confirmed by taking a 200  $\mu$ L aliquot of the headspace and injecting it into the GC for the analysis. The reactor was injected with the internal standard (200  $\mu$ L  $CH_4$ ) and known amount of CO and  $H_2$ , and allowed to equilibrate with the reactant mixture for 15 minutes. Subsequently, a 200  $\mu$ L aliquot of the headspace was sampled and injected into the GC for the analysis. After adding additional known amount of CO and  $H_2$  into the reactor, the sampling of headspace and analysis with GC was continued to complete the full calibration curve. The calibration curve was created from taking the ratio of the integrated areas between the internal standard and generated gases (CO:  $CH_4$  and  $CH_2$ ).

Post-catalysis <sup>1</sup>H and <sup>13</sup>C-NMR studies of the liquid phase were complicated by decomposition products of the sacrificial hole scavenger but did not indicate the presence of other common CO<sub>2</sub> reduction products, such as methanol or formate.

#### Conflicts of interest

There are no conflicts of interest to declare.

## Acknowledgements

This work was supported by NSF (CBET-1804412) and the Welch foundation (A-1639 and A-1880).

#### Notes and references

1 K. E. Dalle, J. Warnan, J. J. Leung, B. Reuillard, I. S. Karmel and E. Reisner, *Chem. Rev.*, 2019, **119**, 2752–2875.

- 2 H. Rao, C.-H. Lim, J. Bonin, G. M. Miyake and M. Robert, J. Am. Chem. Soc., 2018, 140, 17830–17834.
- 3 M. F. Kuehnel, C. D. Sahm, G. Neri, J. R. Lee, K. L. Orchard, A. J. Cowan and E. Reisner, *Chem. Sci.*, 2018, **9**, 2501–2509.
- 4 X. Zhang, M. Cibian, A. Call, K. Yamauchi and K. Sakai, *ACS Catal.*, 2019, **9**, 11263–11273.
- 5 W.-H. Zhang, S. W. Chien and T. A. Hor, *Coord. Chem. Rev.*, 2011, 255, 1991–2024.
- 6 S. Lian, M. S. Kodaimati, D. S. Dolzhnikov, R. Calzada and E. A. Weiss, J. Am. Chem. Soc., 2017, 139, 8931–8938.
- 7 M. F. Kuehnel, K. L. Orchard, K. E. Dalle and E. Reisner, J. Am. Chem. Soc., 2017, 139, 7217–7223.
- 8 Z. Chai, Q. Li and D. Xu, RSC Adv., 2014, 4, 44991-44995.
- 9 H. Lu, Z. Huang, M. S. Martinez, J. C. Johnson, J. M. Luther and M. C. Beard, *Energy Environ. Sci.*, 2020, **13**, 1347–1376.
- 10 G. Neri, M. Forster, J. J. Walsh, C. Robertson, T. Whittles, P. Farràs and A. J. Cowan, *Chem. Commun.*, 2016, 52, 14200–14203.
- 11 N. Ikuta, S.-y. Takizawa and S. Murata, *Photochem. Photobiol. Sci.*, 2014, **13**, 691–702.
- 12 P. L. Cheung, S. C. Kapper, T. Zeng, M. E. Thompson and C. P. Kubiak, *J. Am. Chem. Soc.*, 2019, **141**, 14961–14965.
- 13 S. Lian, M. S. Kodaimati and E. A. Weiss, *ACS Nano*, 2018, **12**, 568–575.
- 14 H.-Y. Chen, T.-Y. Chen, E. Berdugo, Y. Park, K. Lovering and D. H. Son, J. Phys. Chem. C, 2011, 115, 11407–11412.
- 15 M. A. White, A. L. Weaver, R. Beaulac and D. R. Gamelin, ACS Nano, 2011, 5, 4158–4168.

- 16 D. Parobek, T. Qiao and D. H. Son, J. Chem. Phys., 2019, 151, 120901.
- 17 Y. Dong, D. Rossi, D. Parobek and D. H. Son, *ChemPhysChem*, 2016, 17, 660–664.
- 18 Y. Dong, D. Parobek, D. Rossi and D. H. Son, *Nano Lett.*, 2016, **16**, 7270–7275.
- 19 Y. Dong, J. Choi, H.-K. Jeong and D. H. Son, *J. Am. Chem. Soc.*, 2015, **137**, 5549–5554.
- 20 C.-H. Hsia, A. Wuttig and H. Yang, *ACS Nano*, 2011, 5, 9511–9522.
- 21 J. D. Froehlich and C. P. Kubiak, *Inorg. Chem.*, 2012, 51, 3932–3934.
- 22 J. P. Collin, A. Jouaiti and J. P. Sauvage, *Inorg. Chem.*, 1988, 27, 1986–1990.
- 23 C. A. Craig, L. O. Spreer, J. W. Otvos and M. Calvin, J. Phys. Chem., 1990, 94, 7957–7960.
- 24 L. Zhang, D. Zhu, G. M. Nathanson and R. J. Hamers, *Angew. Chem. Int. Ed.*, 2014, **53**, 9746–9750.
- 25 J.-P. Collin, A. Jouaiti and J.-P. Sauvage, *Inorg. Chem.*, 1988, 27, 1986–1990.
- 26 C.-H. Hsia, A. Wuttig and H. Yang, *ACS Nano*, 2011, 5, 9511–9522.
- 27 Y. Yang, O. Chen, A. Angerhofer and Y. C. Cao, J. Am. Chem. Soc., 2008, 130, 15649–15661.
- 28 H.-Y. Chen, S. Maiti and D. H. Son, *ACS Nano*, 2012, **6**, 583–591.
- 29 V. A. Vlaskin, C. J. Barrows, C. S. Erickson and D. R. Gamelin, J. Am. Chem. Soc., 2013, 135, 14380–14389.